Title

Ultrastructural analysis of hippocampal pyramidal neurons from apolipoprotein E-deficient mice treated with a cathepsin inhibitor

Journal

Brain Cell Biology, 33(1)

ISSN

1559-7105

Authors

Díaz-Cintra, Sofia
Yong, Alex
Aguilar, Azucena
et al.

Publication Date

2004

DOI

10.1023/b:neur.0000029647.41374.98

Journal of Neurocytology **33**, 37–48 (2004)

Ultrastructural analysis of hippocampal pyramidal neurons from apolipoprotein E-deficient mice treated with a cathepsin inhibitor

SOFIA DÍAZ-CINTRA[1], ALEX YONG[2], AZUCENA AGUILAR[1], XIAONING BI[2,3], GARY LYNCH[3] and CHARLES E. RIBAK[2*]

[1]*Department of Developmental Neurobiology and Neurophysiology, Institute of Neurobiology, University of Mexico, Juriquilla, Querétaro México 76230; Department of* [2]*Anatomy and Neurobiology and* [3]*Psychiatry and Human Behavior, College of Medicine, University of California at Irvine, Irvine, CA 92697-1275*
ribak@uci.edu

Received 10 July 2003; revised 9 September 2003; accepted 11 September 2003

Abstract

Cultured hippocampal slices prepared from apolipoprotein E (apoE)-deficient mice were exposed to an inhibitor of cathepsins B and L and then processed for an ultrastructural analysis of neuronal features for pyramidal cell bodies. Electron microscopy showed that the nuclei of pyramidal cells from treated hippocampal slices were more eccentrically located than those from untreated slices. In addition, increased numbers of vesicles were associated with the Golgi complex while microtubules were less frequent in the proximal dendrites. Consistent with previous studies in rats, treated apoE-deficient slices had increased numbers of lysosomes and multivesicular bodies. Finally, there were reductions in the number of synapses around the cell body, a finding similar to that found in the brains from Alzheimer's disease patients. These results provide ultrastructural data indicating that partial lysosomal dysfunction in apoE-deficient brains rapidly induces characteristic features of the aged human brain.

Introduction

The earliest clinical phase of pathology of Alzheimer's disease (AD) begins with a subtle alteration of the hippocampus involving changes in synaptic efficiency prior to frank neuronal degeneration (Selkoe, 2002). This synaptic dysfunction is hypothesized to result from diffusible oligomeric assemblies of the amyloid beta protein, which form plaques located in the neuropil between the cell bodies of neurons. Neurofibrillary tangles, another pathologic hallmark of AD, are primarily found within the somata and proximal dendrites of telencephalic neurons. Both plaques and tangles have been partially reproduced in several animal models (Gotz *et al.*, 2001; Le *et al.*, 2001; Lewis *et al.*, 2001; Terai *et al.*, 2001). Abnormal phosphorylation of the microtubule binding protein, tau, is regarded as a crucial step in the formation of neurofibrillary tangles. With regard to synaptic changes in AD, a recent quantitative morphometric study of temporal and frontal cortical biopsies, performed within an average of 2–4 years after the onset of clinical AD, revealed a 25 to 35% reduction in the numerical density of synapses (Davies *et al.*, 1987). In accord with this, subsequent studies (Masliah *et al.*, 2001) reported a 25% reduction in synaptophysin-immunoreactive axon terminals in the neocortex and hippocampus. From these observations it follows that changes in the numbers of synapses should be evaluated in AD models.

Previous studies showed that several features of aged brain could be reproduced *in vitro* using hippocampal (Bednarski & Lynch, 1996) and cortical brain slices (Yong *et al.*, 1999) treated with a selective inhibitor of cathepsins B and L, *N*-CBZ-L-phenylalanyl-L-alanine-diazo-methyl-ketone (ZPAD). This treatment experimentally mimics changes in cathepsins during brain aging (Nakanishi *et al.*, 1994). Neurons in these slices exhibit meganeurites, a singular pathology found in aged human brains (Braak, 1979). Meganeurites are accumulatins of lysosomes in the proximal region of the axon near the soma; because of their size, density, and location, meganeurites are assumed to interfere with the integrity of somato-axonal communication (Bednarski *et al.*, 1997; Yong *et al.*, 1999). More recently, Bi *et al.* (2001)

* To whom correspondence should be addressed.

0300–4864

analyzed ZPAD-treated hippocampal slices from the brains of apolipoprotein E (apoE)-deficient mice using the slice culture methods and experimental treatments as in the above experiments. Apo-E-deficient mice differ from wild type in that they are missing an important microtubule-associated protein that protects tau from being hyperphosphorylated and prevents the generation of intracellular neurofibrillary tangles (Strittmatter & Roses, 1996). Immunocytochemical analyses with antibodies against human paired helical filaments revealed the presence of dense intracellular structures in scattered neurons in the subiculum, stratum oriens of hippocampal field CA1, and hilus of the dentate gyrus (Bi *et al.*, 2001). The distribution and appearance of these inclusions agreed with that described for intraneuronal neurofibrillary tangles in early stage AD. Electron microscopy was also used to show twisted filaments in scattered hippocampal cells with small cell bodies and irregular shapes (Bi *et al.*, 2001)

As evident from the light microscopic descriptions of apoE-deficient slices, most neurons in the hippocampal/subicular cell layers (stratum pyramidale, stratum granulosum) do not generate tangle-like structures (Bi *et al.*, 2001). Nonetheless, it seems unlikely that neurons with the same cellular disturbances (apoE deficient, partial lysosomal dysfunction) fall into distinct pathological and non-pathological groups. The present study sampled the stratum pyramidale to test whether neurons in segments of experimentally treated apoE-deficient slices where tangle-like profiles are rare (in light microscopic surveys) nonetheless exhibit features that are prominent in AD.

Methods

Hippocampal slice cultures were prepared using the technique described by Stoppini *et al.* (1991). Briefly, 10 to 13 day old C57B1/6J (wildtype) and C57B1/6J-Apoetm 1Unc (ApoE-deficient) mouse pups (Jackson Laboratory) were killed by decapitation under light isoflurane anesthesia and the hippocampus was dissected out under sterile conditions. Sections of 400 μm thickness were cut perpendicularly to the long axis of the hippocampus using a Mcllwain tissue chopper in cutting medium consisting of MEM with Earle's salts (Gibco, Rockville MD), 25 mM HEPES, 10 mM Tris base, 10 mM glucose, and 3 mM $MgCl_2$ (pH 7.2). The slices were then transferred to the membranes of millicel-CM culture inserts (Millipore Corp.) in six-well culture cluster plates with 2–3 slices per insert, six inserts per culture plate and 1 ml media per well. The upper surfaces of the slices were exposed to humidified 37°C atmosphere containing 5% CO_2. The culture medium was previously described by Bednarski *et al.* (1997). After 12–14 days *in vitro*, the organotypic cultures were incubated with growth medium containing 20 μM N-CBZ-L-phenyalanyl-L-alanine-diazo-methyl-ketone (ZPAD, Bachem Bioscience Inc., Torrance, CA), a selective inhibitor of cathepsins B and L (Green & Shaw, 1981), or vehicle alone (0.01 dimethylsulfoxide) for 6 days. The treatment medium was replenished every 2 days.

For electron microscopy, control and ZPAD treated slices from apoE-deficient mice were fixed in an ice-cold solution of 0.1 M phosphate buffer (pH 7.4), 1.5% paraformaldehyde and 1.5% glutaraldehyde. After 2 hours, this solution was aspirated and slices washed three times in phosphate buffer saline (PBS: 0.1 M phosphate buffer, 0.9% NaCl, pH 7.3). Slices were post-fixed in 2% osmium tetroxide in PB for 1 hour, dehydrated in a series of graded alcohols, and embedded in Polybed-812. Semi-thin (1 μm) sections were cut from these blocks and stained with 0.1% toluidine blue. These sections were used to identify the various regions of the hippocampal slices. The analysis focused on the CA1 region of the hippocampus because the previous results of Bi *et al.* (1999) showed cells containing tangle-like structures in this region. After trimming the specimen to this region, thin sections were cut with a diamond knife, mounted on Formvar-coated slot grids, stained with uranyl acetate and lead citrate, and examined with a Philips CM-10 transmission electron microscope.

DATA COLLECTION, ANALYSIS AND INTERPRETATION

The electron microscopic data were collected by photographing pyramidal cells from the CA1 region of vehicle- or ZPAD-treated hippocampal slices at primary magnifications of 3,900× and enlargements at 11,500×. These somata were identified by their possessing apical and basal dendrites and a large nucleus surrounded by perikaryal cytoplasm indicating that the plane of section was through the central portion of the cell body. The negatives were scanned into a computer using a flatbed scanner and the prints were obtained from a HP Deskjet 990 printer (Hewlett-Packard, USA). For morphometric analyses, the negatives taken at a primary magnification of 3,900× were digitized in a Macintosh computer using the program IpLab (Version 3.6, Scanalystics, Inc., USA). The following analyses were done for each neuron. The areas of the cell body, nucleus and Golgi complex were obtained. Then, the numbers of microtubules, lysosomes, and multivesicular bodies were counted and expressed as the numbers per square micron of perikaryal cytoplasm. The area of the perikaryal cytoplasm was obtained for each neuron by subtracting the area of the nucleus from that of the cell body. Finally, the perimeter of each cell body was measured for expressing the number of axosomatic synapses per unit length of somal surface. In addition, the centers of each cell body and nucleous were determined using a series of Sholl rings, and the distance between the two centers were calculated to determine the extent of nuclear eccentricity. Statistical tests (*e.g.*, ANOVA) were used to determine significant differences between the two groups.

Results

QUALITATIVE ANALYSIS

Many pyramidal-shaped cells from vehicle- or ZPAD-treated hippocampal slices from apoE-deficient mice were identified in thin sections as neurons. These cells exhibited a prominent nucleus, perikaryal cytoplasm with organelles, and a plasma membrane with several axosomatic synapses (Figs. 1 and 2). Both the somata and proximal dendrites of several pyramidal neurons of different sizes were analyzed. Particular attention was

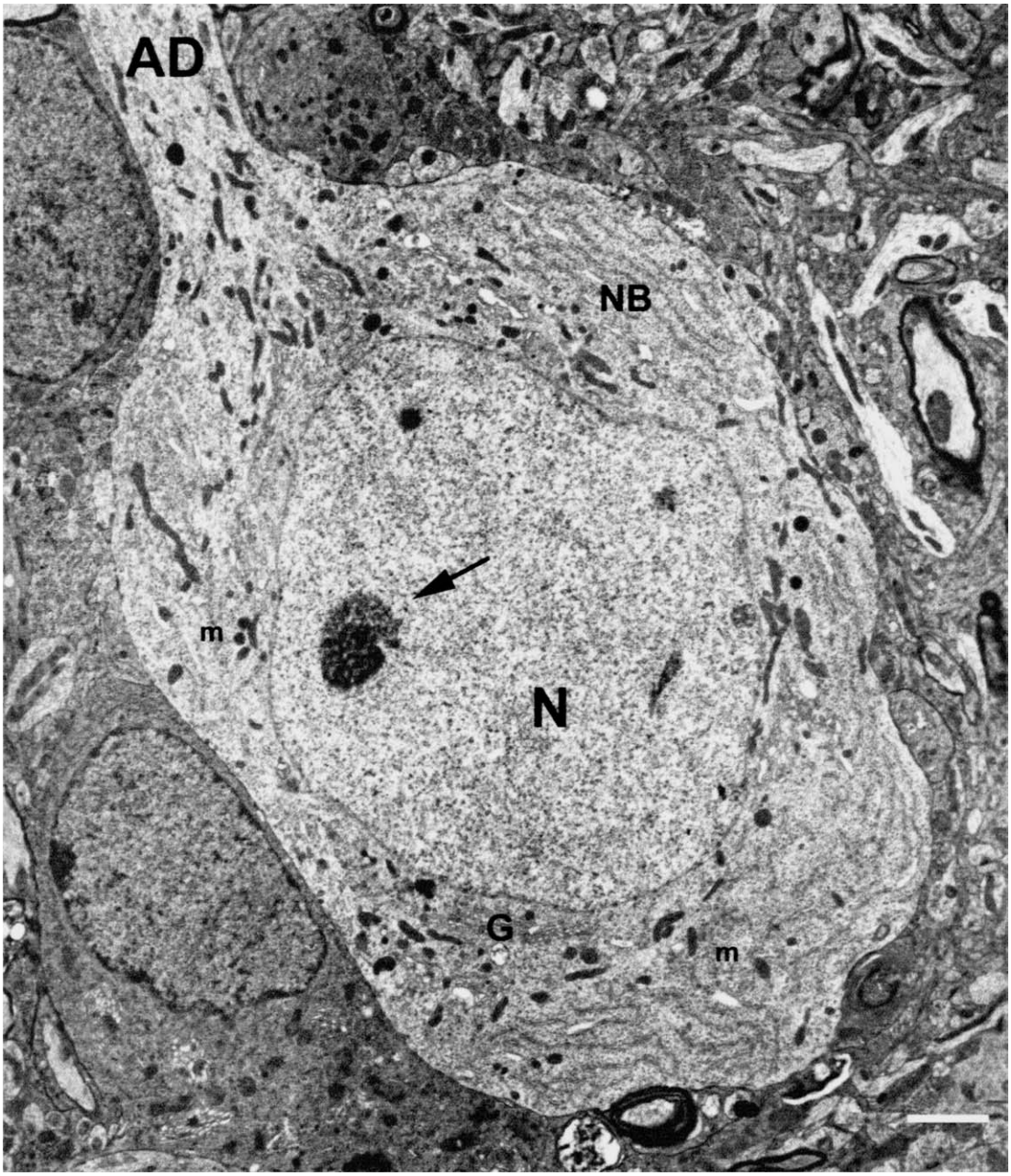

Fig. 1. Electron micrograph of a pyramidal cell from an untreated hippocampal slice. Note the large, centrally-located nucleus (N) and prominent nucleolus (arrow). The perikaryal cytoplasm is enriched with organelles, including Nissl bodies (NB), Golgi complex (G) and many mitochondria (m). An apical dendrite (AD) arises from the upper left corner of this cell body. Scale bar $= 2\ \mu$m.

paid to the structure and numbers of microtubules in the perikaryal and dendritic cytoplasm and the location of the nucleus within the cell body.

The perikarya and dendrites of CA1 pyramidal cells from vehicle-treated hippocampal slices showed the normal features described for hippocampal pyramidal cells (Figs. 1 and 2). The cell bodies had a well-defined, centrally-located nucleus with a prominent nucleolus and various organelles in the perikaryal cytoplasm (Fig. 1). The latter included cisternae of both granular and smooth endoplasmic reticulum, polyribosomes, mitochondria, Golgi complex, lysosomes, multivesicular bodies, microtubules and neurofilaments (Fig. 2A). Axosomatic synapses were also found on the surface of cell bodies (Fig. 2A). The proximal dendrites of these pyramidal cells showed a reduction in most of the organelles except for polyribosomes, microtubules and mitochondria (Fig. 2B and C). Axodendritic shaft and spine synapses were also observed.

Hippocampal pyramidal cells from ZPAD-treated slices had several changes in their cell bodies as compared to those from vehicle-treated slices. The most

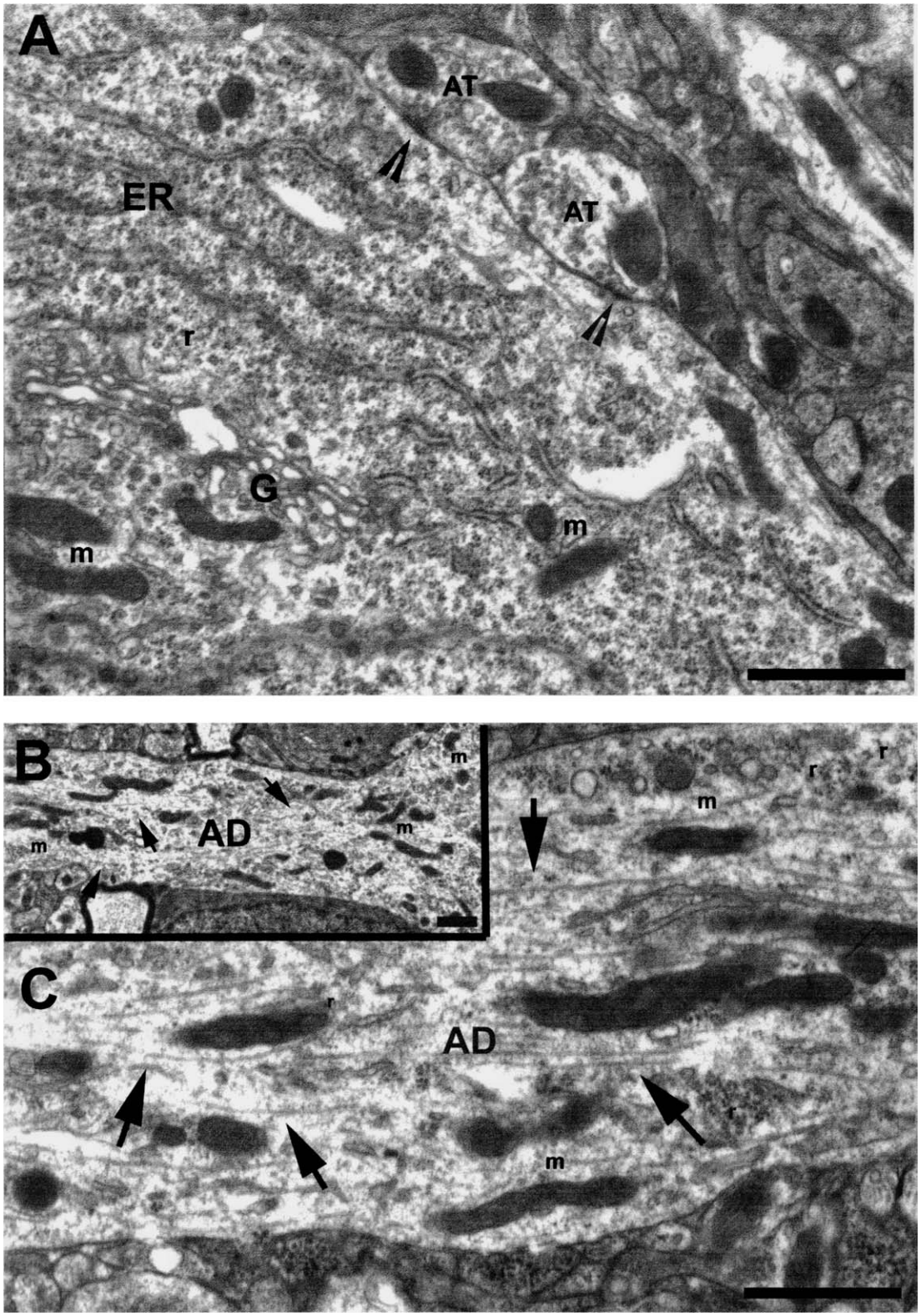

Fig. 2. Enlargements of the pyramidal cell shown in Figure 1 to illustrate parts of the cell body and apical dendrite. (A) shows a portion of the cell body with several typical organelles including the granular endoplasmic reticulum (ER), Golgi complex (G), microtubules and mitochondria (m). Note that two adjacent axon terminals (at) form axosomatic synapses (open arrows) with this pyramidal cell. (B and C) show low and high magnifications of the proximal apical dendrite (AD) of this cell (rotated 90 degrees counter clockwise from the orientation in Fig. 1). Several mitochondria (m) and microtubules (arrows) are found in this proximal apical dendrite as well as groups of polyribosomes (r). Scale bars = 1 μm.

evident of these was an eccentrically located nucleus often located close to the plasma membrane (Fig. 3A). These nuclei usually had indentations and clefts, and occasionally took on a dumb-bell shape (Fig. 4A). In an extreme case of nuclear eccentricity, the nucleus appeared in a pouch-like sac contiguous with the side of the pyramidal cell body, with the cell appearing as an octopus with the head region containing the nucleus (not shown). The Golgi complex was enlarged in the perikaryal cytoplam and showed many clear or dense small, round vesicles (Figs. 3 and 4C). The Nissl bodies varied in size, and often their cisternae were dilated more than normal (Figs. 3A and 5C). Microtubules appeared to be reduced in number because some pyramidal cells had clear zones in the perikaryal cytoplasm in which microtubules were altogether absent. A few twisted filaments were sometimes seen in these clear areas (Fig. 5A and B). The number of lysosomes in the nucleus and proximal dendrites was clearly increased above control slices (Figs. 3 and 4), a finding consistent with previous studies of ZPAD-treated hippocampal slices from rats (Bednarski *et al.*, 1997). Possibly related to this, all of the pyramidal cells showed increased numbers of multivesicular bodies.

Clear areas lacking organelles or microtubules were also found in the proximal dendrites of large pyramidal cells (Fig. 4B and C), and in general, the number of microtubules was substantially reduced compared to dendrites from control slices. Shaft and spine synapses were present on the proximal dendrites found in treated slices.

QUANTITATIVE ANALYSIS

The quantitative data were obtained from 15 pyramidal cells from ZPAD-treated hippocampal slices and 12 pyramidal cells from untreated slices. The first feature that was investigated was the eccentrically located nuclei often found in the ZPAD-treated slices (Fig. 3A). The mean distance (x) between the centers of the nucleus and cell body was 2.37 μm (± 0.37) in ZPAD-treated slices and was substantially greater (124%) than that obtained from vehicle-treated slices ($x = 1.06$ μm, ± 0.23, $p < 0.01$, one way ANOVA). These data are shown in Fig. 6. The number of lysosomes per μm^2 of perikaryal cytoplasm was increased by 266% over control ($p < 0.01$, one way ANOVA) as was the incidence of a related organelle, multivesicular bodies ($p < 0.01$, one way ANOVA) by 280% (Fig. 7). Frequency values for microtubules in the perikaryal cytoplasm were reduced (control: 0.38 ± 0.06; experimental: 0.22 ± 0.07) in the ZPAD-treated slices, but this difference did not reach statistical significance (Fig. 7). The percentage of perikaryal cytoplasm occupied by the Golgi complex was increased in the ZPAD-treated slices, as summarized in Figure 8. In addition, there was a large (60%) decrease in the number of axosomatic synapses per μm length of cell body membrane in ZPAD-treated neurons (Fig. 9, control: 0.18 ± 0.06; experimental: 0.07 ± 0.009).

The proximal dendrites of these pyramidal cells also showed changes in their organelles and synapses. Microtubules were reduced in number showing a 78% decrease that was statistically significant ($p < 0.001$), while multivesicular bodies showed a 1300% significant increase ($p < 0.001$) in treated animals (Fig. 10). The number of lysosomes per μm^2 did not show any significant differences (Fig. 10). Finally, there was a large (63%) significant decrease ($p < 0.01$) in the number of axodendritic synapses per μm length of dendritic membrane in ZPAD-treated animals (Fig. 11, control: 0.217 ± 0.04; experimental: 0.08 ± 0.01).

Discussion

This ultrastructural analysis demonstrated that experimentally induced lysosomal dysfunction in apoE-deficient slices produces a number of age-related changes in neurons lacking evident tau pathology: (1) nuclei that were more eccentrically located and more indented, (2) occasional filaments in their perikaryal cytoplasm, (3) increased numbers of lysosomes and multivesicular bodies, (4) reduced numbers of microtubules in the proximal dendrites, and (5) decreased numbers of axosomatic synapses on the cell body.

CHANGES IN CYTOSKELETON

A previous study showed that treatment of hippocampal slices from apoE-deficient mice with ZPAD induced formation of tangle-like structures in scattered, shrunken neurons localized mainly in the stratum oriens of the subiculum and hippocampal field CA1, and in the hilus of the dentate gyrus (Bi *et al.*, 2001). These large, immunopositive structures were rare in the pyramidal and granule cell layers (Bi *et al.*, 2001). The present study indicates that pyramidal cells, while lacking tangle-like profiles, do exhibit a number of cytoskeletal abnormalities. Twisted filaments in clear zones of the perikaryal cytoplasm, though uncommon, were observed in some neurons. Also, the dendrites of several pyramidal cells showed similar clear areas where microtubules should have been present. Together, these changes are suggestive of a gradual breakdown of the cytoskeleton, possibly accompanied in some cells by the earliest stages of tangle formation. Why these effects observed in pyramidal cells do not proceed, within the time frame of testing, to the shrunken and distorted stage seen in stratum oriens cells with intraneuronal tangles is a critical question for future research. Similar heterogeneity is found in AD, where evident tau pathology is restricted to particular regions, and even in those, does not affect all neurons.

Disturbances in the cytoskeleton may be responsible for the abnormal location and distorted appearance of

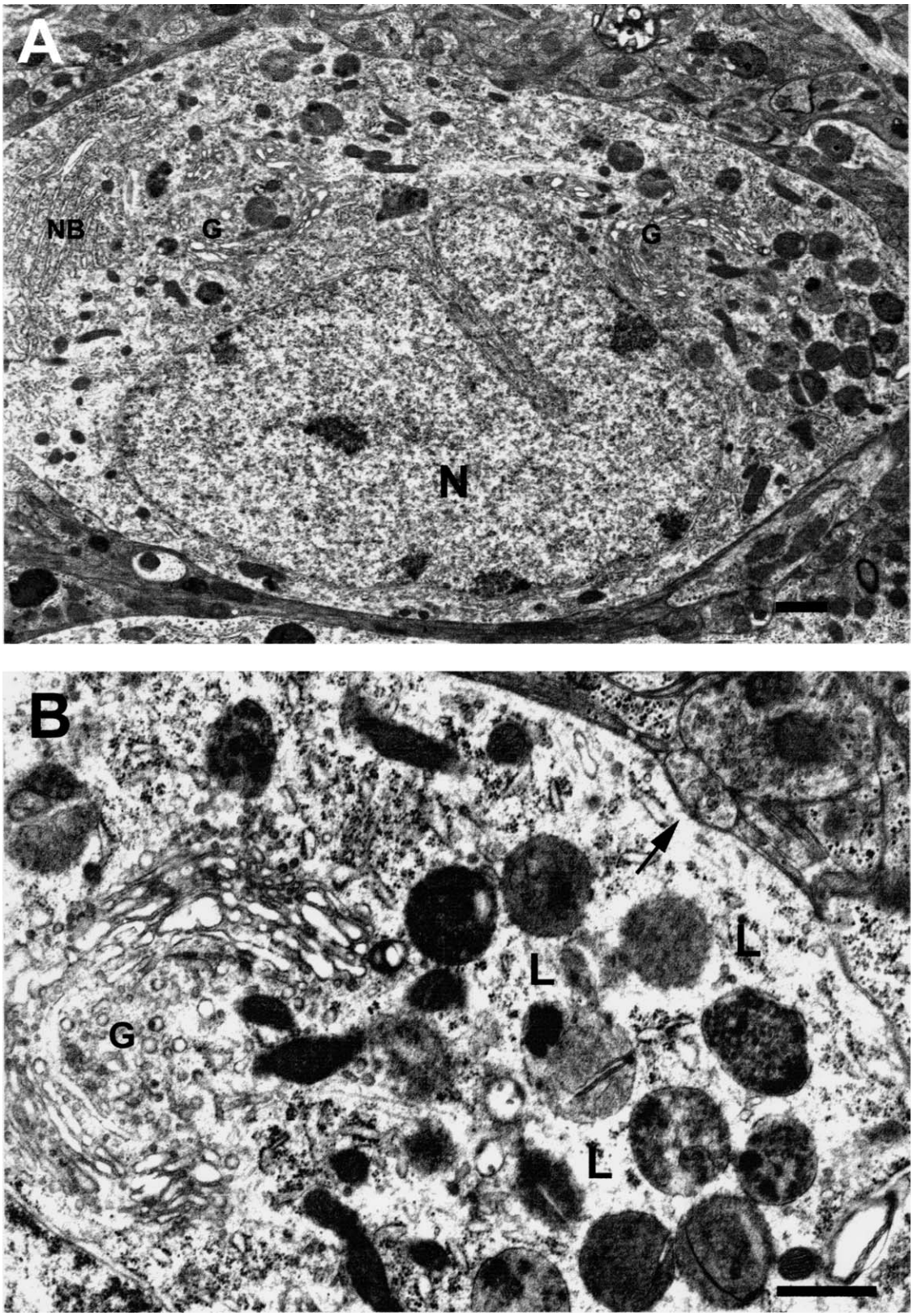

Fig. 3. Electron micrographs of a pyramidal cell from a ZPAD-treated hippocampal slice. (A) shows a neuron with an eccentrically-located nucleus (N) that is infolded. Note that the granular endoplasmic reticulum forms a Nissl body (NB) and that several of its cisternae are dilated (see enlargement in Fig. 5C). The cytoplasm above the nucleus has a clear zone (see Fig. 5A and B). Other parts of the perikaryal cytoplasm contain increased numbers of lysosomes and Golgi complex (G). (B) is an enlargement of the right side of the cell body in A to show lysosomes (L), Golgi complex (G) and an axosomatic symmetric synapse (arrow). Scale bars = 1 μm.

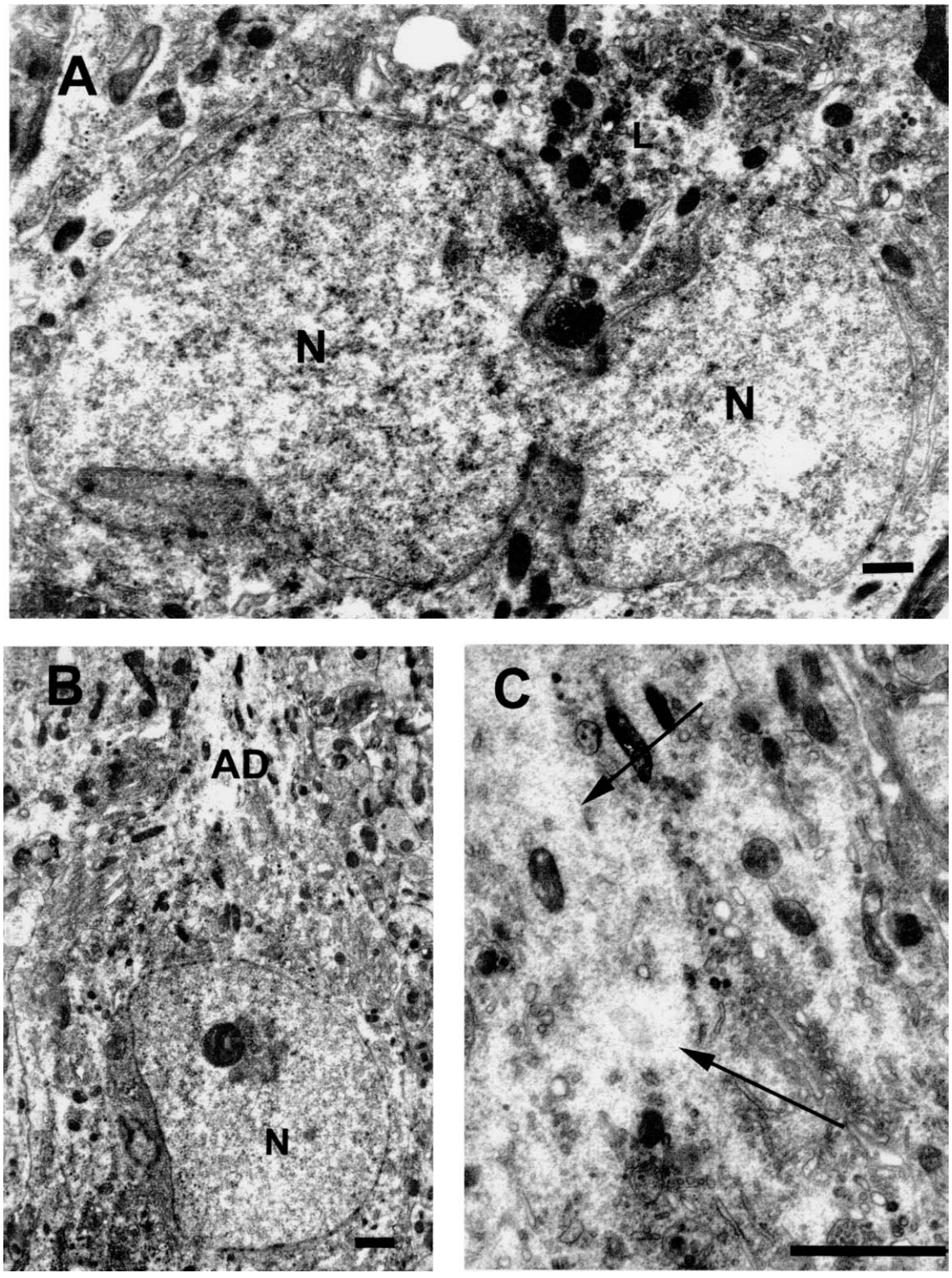

Fig. 4. Electron micrographs of two other pyramidal cells from a ZPAD-treated hippocampal slice. (A) shows that one of the pyramidal cells has a dumbbell-shaped nucleus (N) with deep infoldings that appear to form an unusual bi-lobed structure. (B and C) show another pyramidal cell with a slightly eccentric nucleus (N) and an apical dendrite (AD). Note that the proximal portion of the dendrite in C has clear zones (arrows) where microtubules are lacking and filamentous particles are found. Scale bars $= 1\ \mu$m.

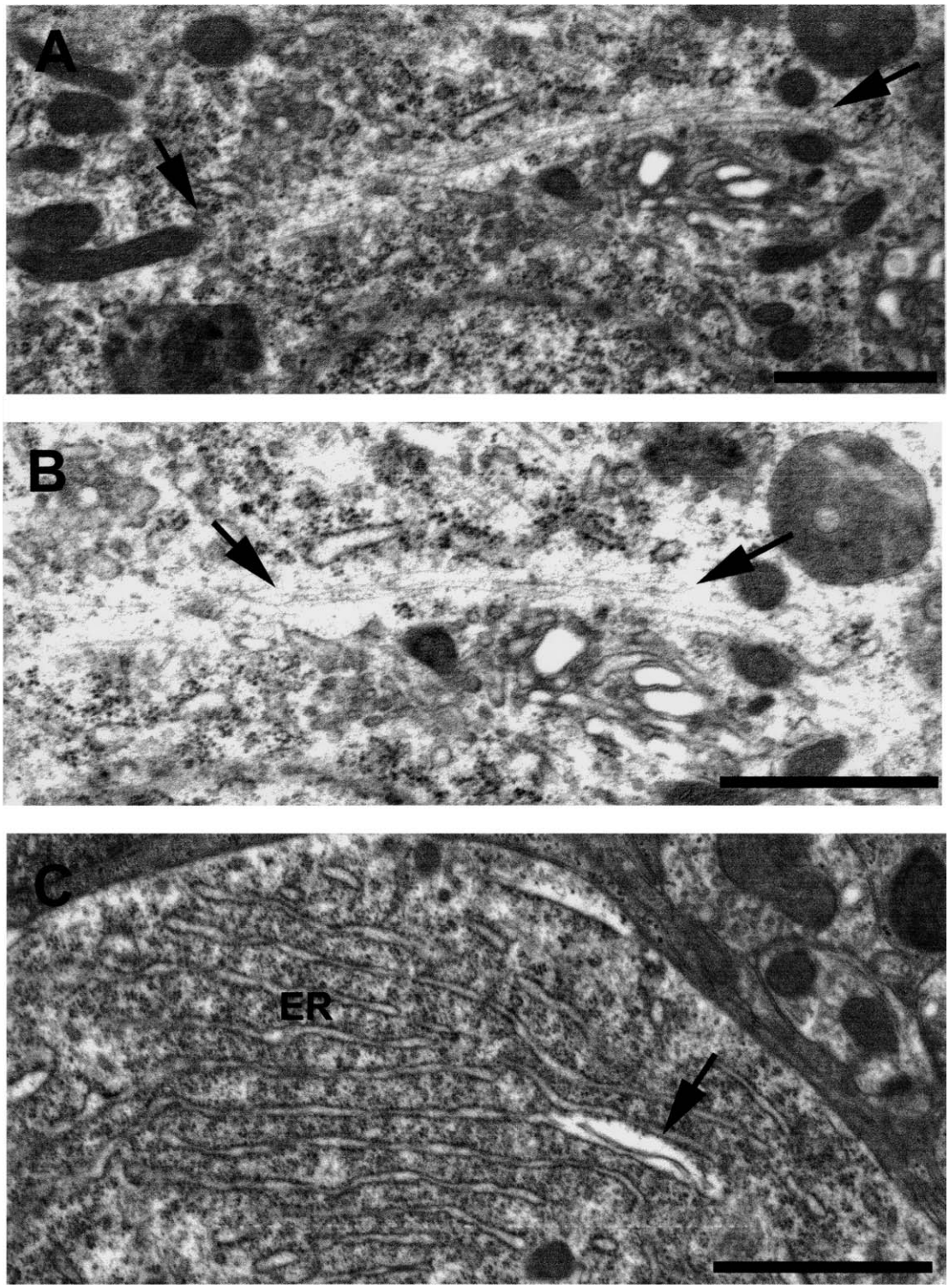

Fig. 5. Enlargements of the pyramidal cell shown in Figure 3 to provide higher resolution images of the organelles in the cell body. (A) shows a portion of the cell body that contains a clear zone (arrows) lacking organelles. (B) is an enlargement of the clear region in A to show the fine filaments that criss-cross each other (arrows). (C) is an enlargement of the granular endoplasmic reticulum (ER) to show several dilated cisternae (arrow) (cf., Fig. 2A). Scale bars = 1 μm.

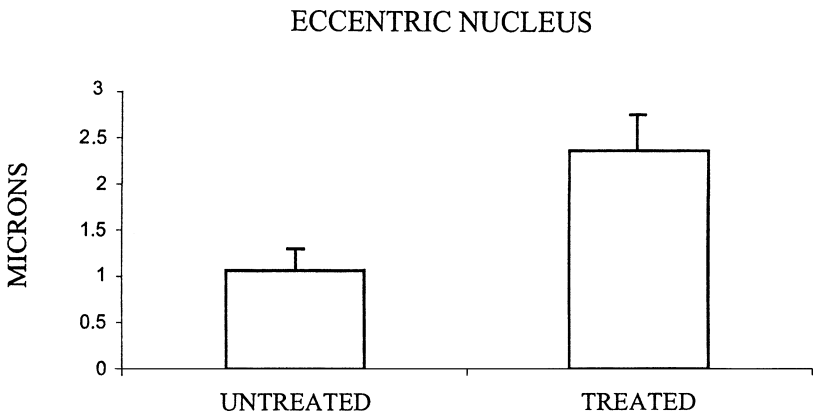

Fig. 6. Histogram to show the significant difference ($p < 0.01$) in eccentricity of the nucleus between untreated and ZPAD-treated hippocampal pyramidal cells. This distance was calculated as the number of microns between the center of the cell body and the center of the nucleus using Sholl rings.

the nuclei in the seemingly intact pyramidal cells. For example, it has been proposed that the microtubules in the perikaryal cytoplasm play an important role in contributing to the cytoskeleton of the neuron and maintaining the round shape and central location of nuclei in pyramidal cells (Peters *et al.*, 1991). Changes in the location of nuclei to eccentric positions have been reported after cutting the major axons of neurons in many brain regions, the so-called chromatolytic reaction (Shamboul, 1979). And in the present study, some eccentric nuclei were present and were accompanied by twisted filaments in their cell body's cytoplasm although a significant reduction in microtubules was not found for somata.

PROLIFERATION AND ACCUMULATION OF LYSOSOMES

Previous studies described lysosomal proliferation in rat hippocampal and cortical slices treated with ZPAD (Bednarski *et al.*, 1997; Bi *et al.*, 1999; Yong *et al.*, 1999). Results of the present study on apoE-deficient mouse hippocampal slices are consistent with these observations. Moreover, the magnitude of the increase in lysosomes (about four-fold) appeared to be very similar in the present study relative to that of the previous work. Lysosomal proliferation has been observed in neurons of aged rats and humans and in vulnerable cells in AD (Terry *et al.*, 1964; Brizzee *et al.*, 1969; Brunk & Ericsson, 1972; Hinds & McNelly, 1979; Cataldo *et al.*, 1996). It seems likely that lysosomal hyperplasia in the case of aged humans arises from the same factors that trigger it in the experimental slices. The changes in the Golgi complex and multivesicular bodies are probably associated with those alterations in the lysosome-endosomal system that result in hyperplasia (Cataldo & Nixon, 1990). On the other hand, impairment in intracellular trafficking would also result in an accumulation of organelles in the cell body.

Endoplasmic reticulum and mitochondria are the major elements for maintaining intracellular calcium homeostasis; impairment in the capacity of the calcium buffering system has been hypothesized as a critical step in age-related neurodegeneration. It is noteworthy, then, that the endoplasmic reticulum in ZPAD treated slices exhibited dilated cisternae. The possibility that lysosomal dysfunction in apoE-deficient slices leads to a loss of calcium buffering is currently under investigation.

CHANGES IN AXOSOMATIC SYNAPSES

The synaptic defects in the hippocampus of individuals with AD correlate with the severity of cognitive impairment (Sze *et al.*, 1997). Evidence for a substantial loss of inhibitory synapses in AD has been described (Soricelli *et al.*, 1996). It is interesting to note that a decrease in the number of axosomatic synapses was found in the ZPAD-treated slices relative to control slices. Most axosomatic synapses for hippocampal pyramidal cells arise from interneurons (Freund & Buzsaki, 1996) that are known from physiological studies to survive slice preparation. Decreases in the numbers of axosomatic synapses in the field CA1 of ZPAD treated hippocampal slices could result from axonal/neuronal degeneration of interneurons in this region. Alternatively, changes in the cytoskeletal system could result in the loss of structures needed to anchor synaptic specializations.

SUMMARY

In conclusion, the present study found that experimentally induced lysosomal dysfunction caused a number of changes in the features of neuronal cell bodies and proximal dendrites of typical pyramidal cells from cultured apoE-deficient hippocampal slices. These changes include cytoskeletal abnormalities, eccentricity of the nucleus, lysosomal proliferation and enlargement of the Golgi complex and the

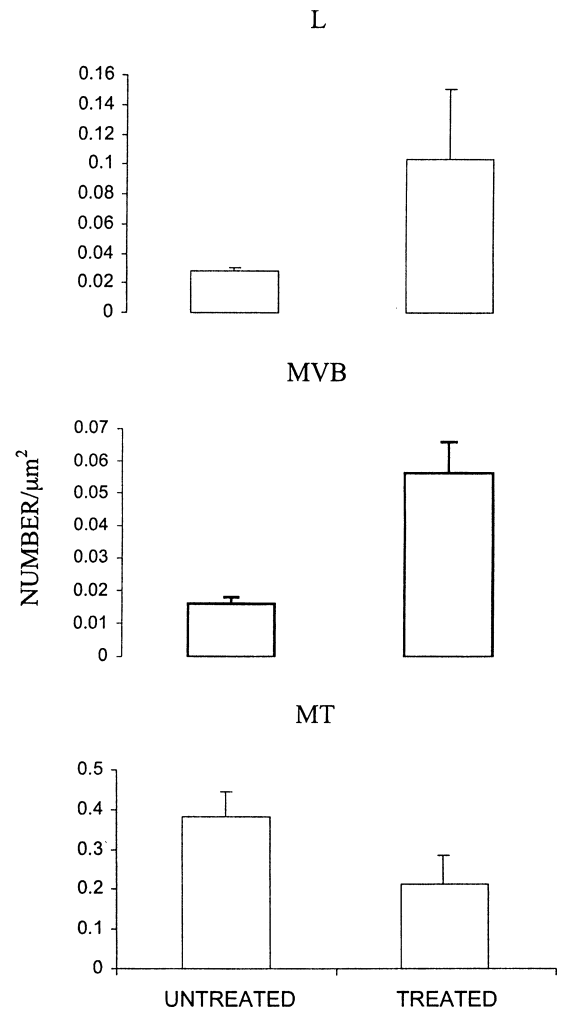

Fig. 7. Histograms to show differences in organelles found in the perikaryal cytoplasm of pyramidal cells from untreated and ZPAD-treated hippocampal slices. The numbers per unit area of both lysosomes (L) and multivesicular bodies (MVB) were significantly increased ($p < 0.002$) in the treated slices. In contrast, the numbers of microtubules (MT) per μm^2 of cytoplasm were decreased in treated slices but the difference was not significant.

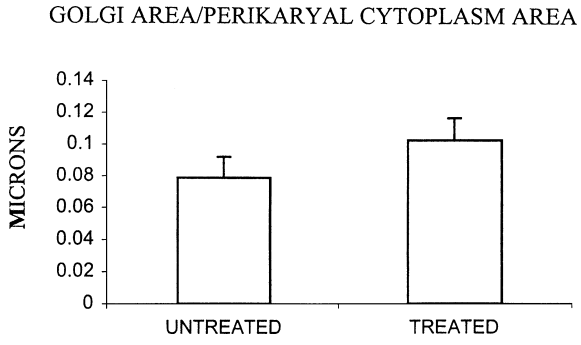

Fig. 8. Histogram showing the amount of area occupied by the Golgi complex in the perikaryal cytoplasm of pyramidal cells from untreated and ZPAD-treated hippocampal slices. The ZPAD-treated slices had a 30% significant increase in the area of the Golgi complex.

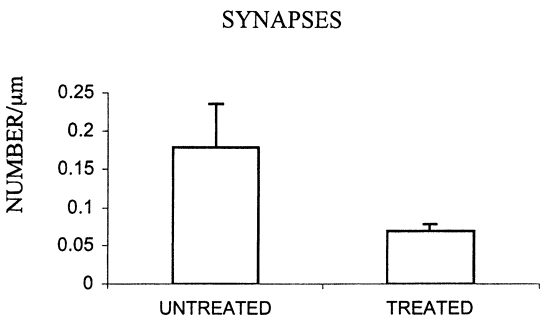

Fig. 9. Histogram of the numbers of axosomatic synapses per unit length of somal surface for pyramidal cells from untreated and ZPAD-treated hippocampal slices. The ZPAD-treated cells showed a 60% significant reduction ($p < 0.004$) in the number of axosomatic synapses.

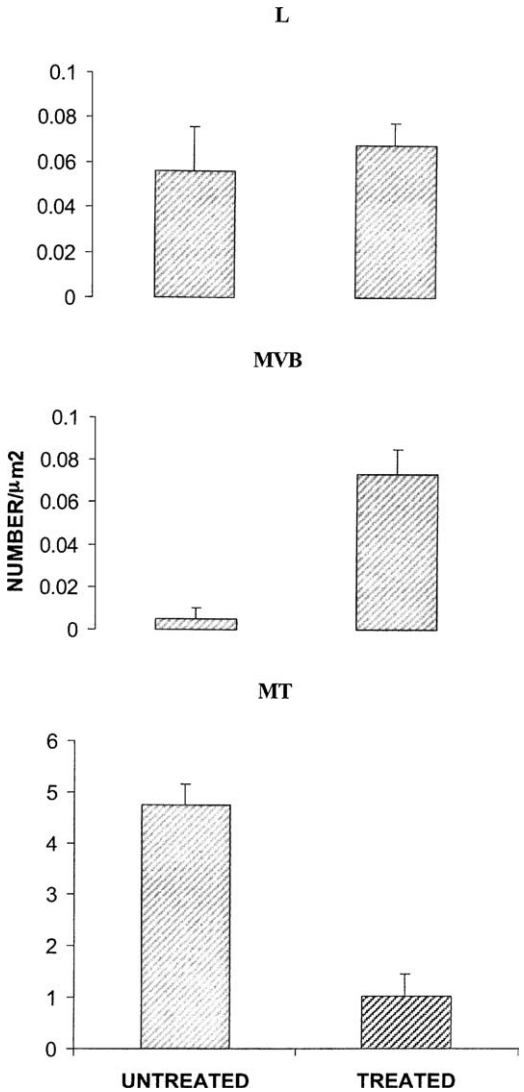

Fig. 10. Histograms of the number of lysosomes (L), multivesicular bodies (MVB) and microtubules (MT) per micron^2 of proximal dendritic cytoplasm. Note that the numbers per unit area of both MVB & MT were significantly changed ($p < 0.001$) in ZPAD-treated slices, but the increase in the numbers of L was not significant.

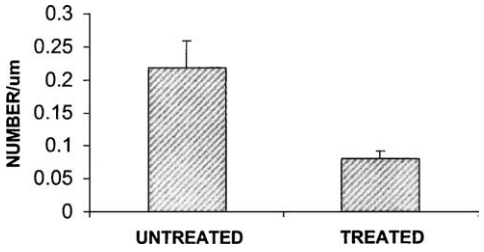

Fig. 11. Histogram of the numbers of axodendritic synapses per unit length of proximal apical dendrite for pyramidal cells from untreated and ZPAD-treated hippocampal slices. The decrease in synapses in the ZPAD-treated cells was significant ($p < 0.01$).

cisternae of endoplasmic reticulum, and loss of axosomatic synapses. These findings indicate that cytoskeletal abnormalities and other age-related changes are widespread in the apoE-deficient, lysosomal dysfunction model rather than being restricted to cells with intraneuronal tangles.

Acknowledgments

The authors gratefully acknowledge Dr. Khashayar Dashtipour and Ms. Marieta Leonor for assistance with the electron microscopy, Leopoldo Gonzalez Santos for assistance with the morphometric analysis, and Tonatzin Pineda and Matthew Korn for technical assistance. This work was supported by National Institute of Aging Grant AG00538 and a grant from the California State Alzheimer's Disease Fund.

References

BEDNARSKI, E. & LYNCH, G. (1996) Cytosolic proteolysis of tau by cathepsin D in hippocampus following suppression of cathepsins B and L. *Journal of Neurochemistry* **67**, 1846–1855.

BEDNARSKI, E., RIBAK, C. E. & LYNCH, G. (1997) Suppression of cathepsins B and L causes a proliferation of lysosomes and the formation of meganeurites in hippocampus. *Journal of Neuroscience* **17**, 4006–4021.

BI, X., YONG, A. P., ZHOU, J., RIBAK, C. E. & LYNCH, G. (2001) Rapid induction of intraneuronal neurofibrillary tangles in apolipoprotein E-deficient mice. *Proceedings of the National Academy of Science, USA* **98**, 8832–8837.

BI, X., ZHOU, J. & LYNCH, G. (1999) Lysosomal protease inhibitors induce meganeurites and tangle-like structures in entorhinohippocampal regions vulnerable to Alzheimer's disease. *Experimental Neurology* **158**, 312–327.

BRAAK, H. (1979) Spindle-shaped appendages of IIIab-pyramids filled with lipofuscin: A striking pathological change of senescent human isocortex. *Acta Neuropathologica (Berlin)* **46**, 197–202.

BRIZZEE, K. R., CANCILLA, P. A., SHERWOOD, N. & TIMIRAS, P. S. (1969) The amount and distribution of pigments in neurons and glia of the cerebral cortex. Autofluorescent and ultrastructural studies. *Journal of Gerontology* **24**, 127–135.

BRUNK, U. & ERICSSON, J. L. (1972) Electron microscopical studies on rat brain neurons. Localization of acid phosphatase and mode of formation of lipofuscin bodies. *Journal of Ultrastructural Research* **38**, 1–15.

CATALDO, A. M. & NIXON, R. A. (1990) Enzymatically active lysosomal proteases are associated with amyloid deposits in Alzheimer brain. *Proceedings of the National Academy of Sciences, USA* **87**, 3861–3865.

CATALDO, A. M., HAMILTON, D. J., BARNETT, J. L., PASKEVICH, P. A. & NIXON, R. A. (1996) Properties of the endosomal-lysosomal system in the human central nervous system: Disturbances mark most neurons in populations at risk to degenerate in Alzheimer's disease. *Journal of Neuroscience* **16**, 186–199.

DAVIES, C. A., MANN, D. M., SUMPTER, P. Q. & YATES, P. O. (1987) A quantitative morphometric analysis of the neuronal and synaptic content of the frontal and temporal cortex in patients with Alzheimer's disease. *Journal of Neurological Sciences* **78**, 151–164.

FREUND, T. F. & BUZSAKI, G. (1996) Interneurons of the hippocampus. *Hippocampus* **6**, 347–470.

GOTZ, J., CHEN, F., VAN DORPE, J. & NITSCH, R. M. (2001) Formation of neurofibrillary tangles in P301L tau transgenic mice induced by Aβ42 fibrils. *Science* **293**, 1491–1495.

GREEN, G. D. & SHAW, E. (1981) Peptidyl diazomethyl ketones are specific inactivators of thiol proteinases. *Journal of Biological Chemistry* **256**, 1923–1928.

HINDS, J. W. & McNELLY, N. A. (1979) Aging in the rat olfactory bulb: Quantitative changes in mitral cell organelles and somato-dendritic synapses. *Journal of Comparative Neurology* **184**, 811–820.

LE, R., CRUZ, L., URBANC, B., KNOWLES, R. B., HSIAO-ASHE, K., DUFF, K., IRIZARRY, M. C., STANLEY, H. E. & HYMAN, B. T. (2001) Plaque-induced abnormalities in neurite geometry in transgenic models of Alzheimer disease: Implications for neural system disruption. *Journal of Neuropathology and Experimental Neurology* **60**, 753–758.

LEWIS, J., DICKSON, D. W., LIN, W. L., CHISHOLM, L., CORRAL, A., JONES, G., YEN, S. H., SAHARA, N., SKIPPER, L., YAGER, D., ECKMAN, C., HARDY, J., HUTTON, M. & MCGOWAN, E. (2001) Enhanced neurofibrillary degeneration in transgenic mice expressing mutant tau and APP. *Science* **293**, 1446–1447.

MASLIAH, E., MALLORY, M., ALFORD, M., DETERESA, R., HANSEN, L. A., MCKEEL, D. W., JR. & MORRIS, J. C. (2001) Altered expression of synaptic proteins occurs early during progression of Alzheimer's disease. *Neurology* **56**, 127–129.

NAKANISHI, H., TOMINAGA, K., AMANO, T., HIROTSU, I., INOUE, T. & YAMAMOTO, K. (1994) Age-related changes in activities and localizations of cathepsins D, E, B, and L in the rat brain tissues. *Experimental Neurology* **126**, 119–128.

PETERS, A., PALAY, S. L. & WEBSTER, H. DE F. (1991) *The Fine Structure of the Nervous System*. New York: Oxford University Press.

SELKOE, D. J. (2002) Alzheimer's disease is a synaptic failure. *Science* **298**, 789–791.

SHAMBOUL, K. M. (1979) Retrograde axon reaction in the lateral vestibular nucleus of neonatal and adult rats. *Journal of Anatomy* **129**, 225–233.

SORICELLI, A., POSTIGLIONE, A., GRIVET-FOJAJA, M. R., MAINENTI, P. P., DISCEPOLO, A., VARRONE, A., SALVATORE, M. & LASSEN, N. A. (1996) Reduced cortical distribution volume of iodine-123 iomazenil in Alzheimer's disease as a measure of loss of synapses. *European Journal of Nuclear Medicine* **23**, 1323–1328.

STOPPINI, L., BUCHS, P. A. & MULLER, D. (1991) A simple method for organotypic cultures of nervous tissue. *Journal of Neuroscience Methods* **37**, 173–182.

STRITTMATTER, W. J. & ROSES, A. D. (1996) Apolipoprotein E and Alzheimer's disease. *Annual Review of Neuroscience* **19**, 53–77.

SZE, C. I., TRONCOSO, J. C., KAWAS, C., MOUTON, P., PRICE, D. L. & MARTIN, L. J. (1997) Loss of the presynaptic vesicle protein synaptophysin in hippocampus correlates with cognitive decline in Alzheimer disease. *Journal of Neuropathology and Experimental Neurology* **56**, 933–944.

TERAI, K., IWAI, A., KAWABATA, S., TASAKI, Y., WATANABE, T., MIYATA, K. & YAMAGUCHI, T. (2001) beta-amyloid deposits in transgenic mice expressing human Beta-amyloid precursor protein have the same characteristics as those in Alzheimer's disease. *Neuroscience* **104**, 299–310.

TERRY, R. D., GONATAS, N. K. & WEISS, M. (1964) The ultrastructure of the cerebral cortex in Alzheimer's disease. *Transactions of the American Neurology Association* **89**, 12.

YONG, A. P., BEDNARSKI, E., GALL, C. M., LYNCH, G. & RIBAK, C. E. (1999) Lysosomal dysfunction results in lamina-specific meganeurite formation but not apoptosis in frontal cortex. *Experimental Neurology* **157**, 150–160.